RESEARCH ARTICLE

Synthesis, Pharmacological Evaluation, and Docking Studies of Ethyl Coumarilate Derivatives as Potential Anti-bladder Cancer in a Mouse Model

AK Khalaf*, OA Omar

Department of Chemistry, College of Science, University of Mosul, Mosul, Iraq.

Received: 10th October, 2023; Revised: 18th October, 2023; Accepted: 19th November, 2023; Available Online: 25th December, 2023

ABSTRACT

In our study, we performed the green synthesis of twenty-one new organic compounds derived from ethyl coumarilate and treated with ammonia derivatives, such as hydrazine, phenylhydrazine, semicarbazide, and thiosemicarbazide. These reactions yielded a five-member ring incorporating benzofuran, and similar reactions with urea, thiourea, and guanidine produced a six-member ring incorporating benzofuran. All compounds were synthesized in our previous work1 and evaluated for their effects on bladder cancer in experimental mice using docking analysis. Among these twenty-one compounds, we selected five based on docking program analysis. These five compounds showed the highest negative ΔG value, indicating strong interaction and effective inhibition of three important enzymes, TNF-alpha, COX-2, and IL-6, responsible for inflammation in the body. The results demonstrated that the prepared organic compounds exhibited robust binding and inhibition towards these enzymes. Subsequently, a study was conducted on 85 male mice, divided equally into seven groups, with each group consisting of five mice. The control group received a normal diet and distilled water, while groups 2 to 7 were administered doses of N-butyl-N-(4-hydroxybutyl) nitrosamine (BBN) at a dose of 0.05% in drinking water for four months. Groups 3 to 7 received intraperitoneal injections of compounds A, B, C, D, and E at three different doses (0.5-1-1.5 mg/kg) for 21 days. Unfortunately, all the mice in group 7 died when this compound was used, possibly due to its high dose. Biochemical results revealed that compound B exhibited intriguing anticancer activity, reducing TNF-alpha levels and inhibiting COX-2 and IL-6 enzymes, reversing bladder cancer injury. Moreover, histopathological examination indicated significant improvement, with the complete disappearance of cancer in the bladder caused by compound B.

Keywords: Ethyl Coumarilate, Phenylhydrazine, Benzofuran, N-butyl-N-(4-hydroxy butyl) Nitrosamine (BBN).

International Journal of Drug Delivery Technology (2023); DOI: 10.25258/ijddt.13.4.66

How to cite this article: Khalaf KA, Omar AO. Synthesis, Pharmacological Evaluation, and Docking Studies of Ethyl Coumarilate Derivatives as Potential Anti-bladder Cancer in a Mouse Model. International Journal of Drug Delivery Technology. 2023;13(4):1548-1556.

Source of support: Nil.

Conflict of interest: None

INTRODUCTION

Cancer is a serious disease that occurs due to abnormal and uncontrolled growth of cells in the body.[1,2] And can be treated through various methods, including chemotherapy,[3] which involves the use of chemical compounds to attack and kill cancer cells by administering chemical doses of organic compounds to the body.[4] The goal of chemotherapy is to reduce the size of the cancerous tumor and destroy any remaining cancer cells.[5] In this study, we have prepared new organic compounds derived from benzofuran, which are known for their various biological effects, including anti-inflammatory. [6] anti-Alzheimer's.[7] and anticancer properties[8]. These organic compounds were theoretically studied using the MCULE docking program to evaluate their effectiveness on specific proteins by calculating the G value and generating 2D and 3D images of the interactions between the enzyme and the compound.[9] The types and numbers of bonds vary from one compound to another. Based on these results, we applied these compounds scientifically to bladder cancer by inducing bladder cancer in mice using the BBN compound through drinking water.[10] We then converted the compounds into different chemical doses and applied them to mice to study the biochemical signals and perform tissue analysis. It was found that the newly derived compounds from benzofuran have a clear impact on bladder cancer. The objective of this study is to evaluate and test the impact of novel chemical compounds

Author for Correspondence: karm.21scp47@student.uomosul.edu.iq

on the levels of three enzymes (TNF-a, COX-2, IL-6) in the serum of white mice with bladder cancer induced by BBN, the compounds were theoretically studied using the program MCULE docking, which revealed a binding interaction between the enzymes and these compounds. Additionally, histological analysis was conducted to assess tissue changes, along with monitoring the levels of the enzymes throughout the study.

Molecular Docking Analysis

The binding orientations and interactions of the potent antitumor derivatives (A, B, C, D, and E) as shown in Figure 1. into three anti-inflammation tumor-regulating proteins, namely TNF-a, COX-2, and IL-6, were simulated using MCULE docking and BIOVIA discovery studio (2021) software. 'The selected proteins' three-dimensional structure (3D) was downloaded from the PDB website. proteins were added with ligands in the mcule docking.[11] The mcule docking specializes in analyzing and evaluating biological activity by using the novel chemical compound of interest and selecting the enzymes for studying their interaction.[12] These enzymes are chosen from the available enzyme database (BDP). Mcule assesses the binding strength between the chemical compound and the selected enzymes by calculating the interaction's ΔG value (free energy) as shown in Table 1. The ΔG value helps estimate the interaction strength and its potential impact on the enzyme. Additionally, Mcule docking can provide 2D and 3D images of the binding that occurred between the prepared chemical compound and the enzyme as part of the result reports as shown in Figures 2-4.[13] The objective of this study is to evaluate and test the impact of novel chemical compounds on the levels of three enzymes (TNF-a, COX-2, IL-6) in the serum of white mice with bladder cancer induced by BBN. The compounds were theoretically studied using the program MCULE docking, which revealed a binding interaction between the enzymes and these compounds. Additionally, histological analysis was conducted to assess tissue changes, along with monitoring the levels of the enzymes throughout the study.

MATERIALS AND METHODS

Chemical Material Used

In this study, standard kits were used to measure the level of (TNF-a, COX-2, and IL-6) in serum was the ELISA technique using ready-made solutions (Kit) according to the manufacturer (Sunlong/China).

Table 1: Binding energies of the potent anti-inflammation derivatives (A, B, C, D, and E) with the three examined proteins.

Ligand	*TNF-a [Kcal/mol]*	*COX-2 [Kcal/mol]*	*IL-6 [Kcal/mol]*
A	-6.6	-5.8	-6.2
B	-7.2	-7.3	-7.4
C	-7.1	-6.9	-6.7
D	-5.7	-5.3	-5.9
E	-5.8	-4.7	-5.1

Methods

Preparation of 7-methoxy-2-hydro-2H-benzofuro[3,2-c] pyrazol-3-one (A) and 7-methoxy-3-oxo-2H-benzofuro[3,2-c] pyrazole-2-carboxamide (B) and 7-methoxy-3-oxo-2H-benzofuro[3,2-c] pyrazole-2-carbothioamide (C)

A mixture of Ethyl Coumarilate (1 mmole) with ammonia derivatives like hydrazine hydrate (99%) or thiosemicarbazide or semicarbazide hydrochloride (5 mmole) in glacial acetic acid (15 ml) The reaction mixture was heated for (3 hours) at (70°C) in Ultrasonic technique with small amount of zirconyl chloride octahydrate ZrOCl2.8H2O as a catalyst. Then, 50 mL) of water was added to the crude mixture, and the solid was collected by vacuum filtration, and washed with warm water. The product was recrystallized from EtOH and dried at room temperature to give compounds (A, C, B)[14-16] as shown in Scheme 1.

Preparation of 2-phenyl-2H-benzofuro[3,2-c] pyrazole-3-one (D)

A mixture of ethyl coumarilate (1 mmole) was dissolved with phenylhydrazine hydrochloride (5 mmole) in dimethyl sulfoxide (DMSO) (10 mL). To this mixture, Piperidine (5 mL) was added dropwise. The reaction mixture was heated for (3 hours) at (70°C) in the Ultrasonic technique with a small amount of zirconyl chloride octahydrate ZrOCl2.8H2O as a catalyst. Then, 50 mL) of water was added to the crude mixture, and the solid was collected by vacuum filtration, and washed with warm water. The product was recrystallized from EtOH and dried at room temperature to give compounds (D)[17] as shown in Scheme 2.

Preparation of 2-thioxo-2H-benzofuro[3,2-d] pyrimidin-4(3H)-one (E)

A mixture of ethyl coumarilate (1 mmole) and thiourea (5 mmole) in glacial acetic acid (15 mL) The reaction mixture was

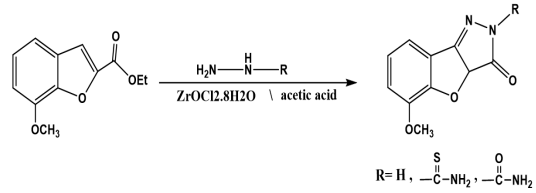

Scheme 1: The synthesis of novel organic compounds A, B, and C

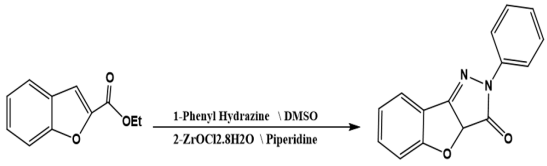

Scheme 2: The synthesis of the novel organic compound D

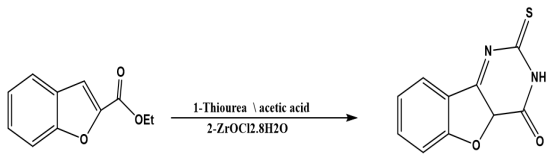

Scheme 3: The synthesis of novel organic compound E

heated for (3 hours) at (70°C) in an Ultrasonic technique with a small amount of zirconyl chloride octahydrate ZrOCl2.8H2O as a catalyst. Then, 50 mL) of water was added to the crude mixture, and the solid was collected by vacuum filtration and washed with warm water. The product was recrystallized from EtOH and dried at room temperature to give compounds (E)[18,19] as shown in Scheme 3.

Animals used

In 85 male mice of weight (25 g) were taken from the animal house of the College of Veterinary Medicine, Mosul University. They were placed in cages equipped and prepared for this purpose and provided with water and animal feed for them. They were divided into seven groups and left for one week to accommodate laboratory light and temperature conditions and then the injection and dosing procedures.

Determining of inducing bladder cancer dose

Determining the dosage for inducing bladder cancer is based on internationally recognized research studies. Following this, a dose of BBN at a concentration of 0.05% was administered over a period of four months by mixing an appropriate quantity of the compound with drinking water for the mice.[20]

Dosage calculation and preparation of a stock solution of novel organic compounds for experimental animals[21]

Stock solutions and doses of novel organic compound (With selected doses, 0.5, 1, and 1.5 mg/kg) as shown in Figure 5 for mice weighing 25 g be calculated as follows.

Body weight of animal =25 g

In a nutshell, 25 g = 0.0375 mg = 0.1 mL of DMSO

The bulk volume of the stock solution required for many animals can be calculated by multiplying both sides by constant value as follows.

$$Dosage\ in(mg) = \frac{Body\ weight\ of\ animal\ (g)}{1000(g)} \times dose(mg)$$

$$Dosage\ in(mg) = \frac{25\ (g)}{1000(g)} \times 1.5(mg) = 0.0375$$

0.0375 mg = 0.1 mL

5 The group of mice

21 the number of days to give a dose.

21 x 5 x 0.0375 mg = 21 x5 x 0.1 mL

3.93mg of novel organic compounds will be dissolved in 10.5 mL of DMSO = x =

Experimental design

$$\frac{3.937(mg)}{10.5\ mL} = 0.374\ mg/mL$$

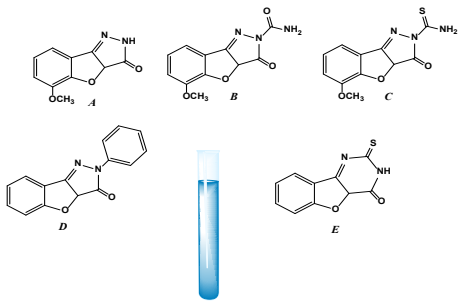

Figure 1: The novel synthesis of heterocyclic compounds.

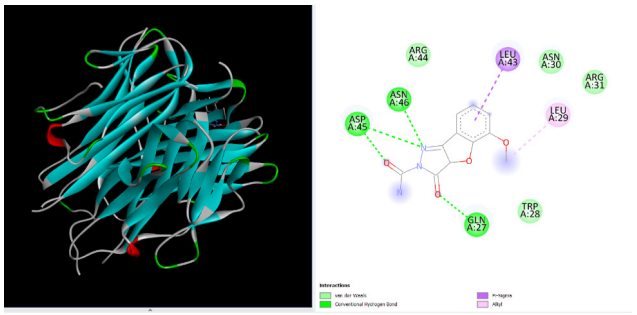

Figure 2: 3D&2D illustration of possible interactions of compound B with the TNF-a protein

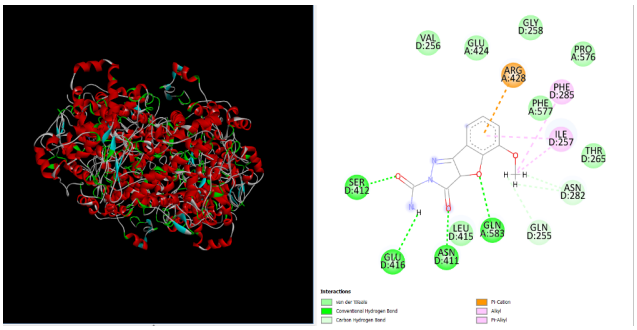

Figure 3: 3D&2D illustration of possible interactions of compound B with the COX-2 protein (PDB ID 1CX2)

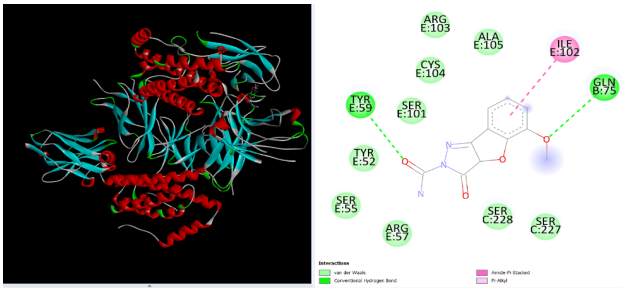

Figure 4: 3D&2D illustration of possible interactions of compound B with the IL-6 protein (PDB ID 5FUC)

Table 2: shows some biochemical variables that were measured in the blood serum of mice treated with (BBN) and A.

B	Control		Mice induced by BBN 0.05%		Dose M6 (0.5mg/kg)		Dose M6 (1 mg/kg)		Dose M6 (1.5 mg/kg)	
	Mean	SD	Mean	SD	Mean	SD	Mean	SD	Mean	SD
IL-6	d 3.95	0.25	a 82.56	0.78	b 6.78	0.19	cd 4.68	0.19	bc 5.99	0.63
TNF-α	c 6.27	0.79	a 460.81	7.91	b 61.69	7.15	c 16.43	2.06	b 73.69	4.18
COX-2	c 12.60	1.07	a 366.91	7.78	b 41.83	0.69	c 15.38	1.48	b 31.25	0.52

The animals were distributed into 7 groups, each including 5 healthy animals, and they were fed a regular diet during the experiment. Another group of animals was dosed daily with (BBN) for a period of 4 months orally. The division of the groups was as follows:

- The first group (Control) received a normal diet throughout the entire experiment.
- The second group was dosed with (BBN) for 4 months and, during the last week, they were additionally administered DMSO.
- The third group was dosed with (BBN) for 4 months, followed by injections of a new synthetic organic compound (A) into the peritoneal cavity for 21 days at doses of 0.5-1-1.5 mg/kg of body weight per day (therapeutic doses).
- The fourth group was dosed with (BBN) for 4 months and then received injections of a new synthetic organic compound (B) into the peritoneal cavity for 21 days at doses of 0.5-1-1.5 mg/kg of body weight per day (therapeutic dose).
- The fifth group was dosed with (BBN) for 4 months and then received injections of a new synthetic organic compound (C) into the peritoneal cavity for 21 days at doses of 0.5-1-1.5 mg/kg of body weight per day (therapeutic dose).
- The sixth group was dosed with (BBN) for 4 months and then received injections of a new synthetic organic compound (D) into the peritoneal cavity for 21 days at doses of 0.5-1-1.5 mg/kg of body weight per day (therapeutic dose).
- The seventh group was dosed with (BBN) for 4 months and then received injections of a new synthetic organic compound (E) into the peritoneal cavity for 21 days at doses of 0.5-1-1.5 mg/kg of body weight per day (therapeutic dose).

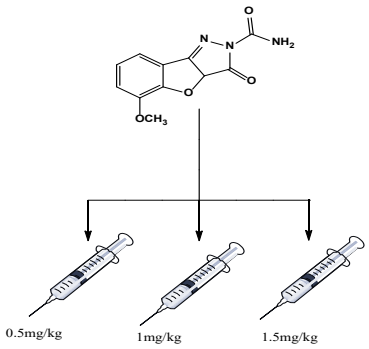

Figure 5: Conversion of the novel organic compound to dose

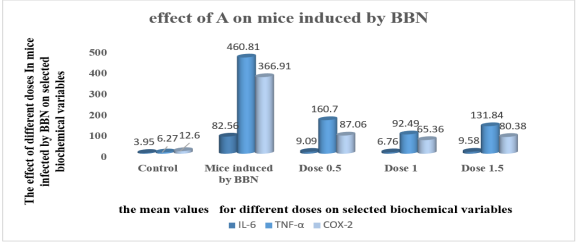

Figure 6: The effect of A on mice induced by BBN

Collection of blood and bladder samples

After completing the experiment, the animals were anesthetized by placing a piece of cotton moistened with ethyl ether directly on the nose for five minutes. Blood was drawn from the eye socket using special capillary tubes, the blood was collected in clean, dry tubes (Plain tubes) free of anticoagulant, then allowed to clot and the serum was separated by centrifuge for 15 minutes at a speed of 5000 cycles/sec. The serum was placed in special tubes for this purpose and kept at a temperature of -20°C until the tests are carried out for the experiment's standards (TNF-a, COX-2, IL-6).

Statistical Analysis

The results were analyzed statistically, where the values of the biochemical variables were described using the mean and standard deviation, and the Duncan Test was used with ANOVA analysis to analyze the impact of the studied biochemical variables.[22]

RESULTS AND DISCUSSION

Results of the biochemical study

Measurement of some biochemical variables in the blood serum
The above values refer to the mean ± standard deviation.
The different letters indicate a significant difference at the probability level P≤0.05.
The above values refer to the mean ± standard deviation.
The different letters indicate a significant difference at the probability level P≤0.05.

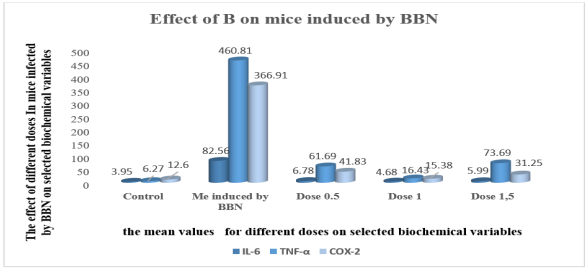

Figure 7: The effect of B on mice induced by BBN

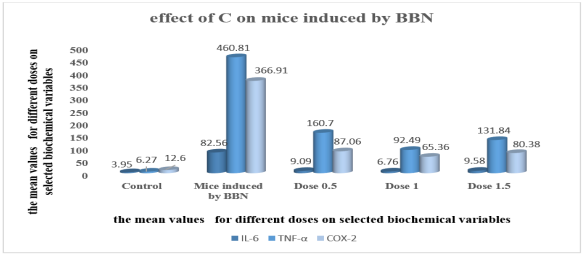

Figure 8: The effect of C on mice induced by BBN

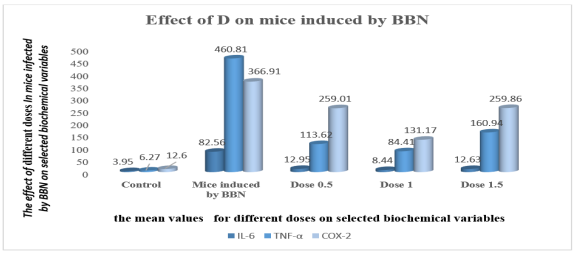

Figure 9: The effect of D on mice induced by BBN

Table 3: Biochemical variables that were measured in the blood serum of mice treated with (BBN) and B.

A	Control		Mice induced by BBN 0.05%		Dose M1 (0.5mg/kg)		Dose M1 (1 mg/kg)		Dose M1 (1.5 mg/kg)	
	Mean	SD	Mean	SD	Mean	SD	Mean	SD	Mean	SD
IL-6	d 3.95	0.25	a 82.56	0.78	b 14.54	0.73	C 7.59	0.44	b 13.88	0.70
TNF-α	d 6.27	0.79	a 460.81	7.91	b 196.25	4.26	D 79.83	7.61	b 207.75	5.55
COX-2	e 12.60	1.07	a 366.91	7.78	c 223.87	5.49	D 117.53	3.08	b 260.17	4.73

Table 4: Biochemical variables that were measured in the blood serum of mice treated with (BBN) and C.

C	Control		Mice induced by BBN 0.05%		Dose M7 (0.5mg/kg)		Dose M7 (1 mg/kg)		Dose M7 (1.5 mg/kg)	
	Mean	SD	Mean	SD	Mean	SD	Mean	SD	Mean	SD
IL-6	d 3.95	0.25	a 82.56	0.78	b 9.09	0.46	c 6.76	0.21	b 9.58	0.22
TNF-α	e 6.27	0.79	a 460.81	7.91	b 160.70	4.72	d 92.49	4.21	c 131.84	4.43
COX-2	d 12.60	1.073	a 366.91	7.78	b 87.06	2.73	c 65.36	1.813	b 80.38	1.73

Table 5: Biochemical variables that were measured in the blood serum of mice treated with (BBN) and D.

D	Control		Mice induced by BBN 0.05%		Dose K2 (0.5mg/kg)		Dose K2 (1 mg/kg)		Dose K2 (1.5 mg/kg)	
	Mean	SD	Mean	SD	Mean	SD	Mean	SD	Mean	SD
IL-6	d 3.95	0.25	a 82.56	0.78	b 12.95	0.58	c 8.44	0.39	b 12.63	0.74
TNF-α	e 6.27	0.79	a 460.81	7.91	c 113.62	5.10	d 84.41	3.28	b 160.94	8.40
COX-2	d 12.60	1.07	a 366.91	7.78	b 259.01	11.13	c 131.17	1.96	b 259.86	6.41

The above values refer to the mean ± standard deviation The different letters indicate a significant difference at the probability level P≤0.05.

The above values refer to the mean ± standard deviation. The different letters indicate a significant difference at the probability level P≤0.05.

Tumor Necrosis Factor (TNF-α) Concentration Level

The findings demonstrated a notable increase, with a probability level of P≤0.05, in the concentration of TNF-α among mice induced with BBN, when compared to the control group as shown in Table 2. This elevation could be ascribed to the activation of immune cells in response to the presence of cancer cells within the bladder.[23] TNF is released by these immune cells as part of the immune response aimed at combating the cancer cells. Moreover, the persistent inflammation commonly associated with bladder cancer can contribute to elevated levels of TNF. This chronic inflammation leads to the production of TNF by immune cells and other cells in the affected area.[24] Notably, the results revealed a significant reduction in TNF-α concentration among mice treated with various doses, specifically A, B, C, and D, when compared to the BBN-induced group due to interaction and inhibition of the enzyme form as shown in Table 5. The notable decrease in TNF-α concentration can be attributed to the remarkable efficacy of compound B in comparison to the other doses shown in Figure 7. This decrease is attributed to the strong binding interactions between the compound and the enzyme, as theoretically predicted by the docking program. There are four hydrogen bonds, along with other types of bonds, contributing to this strong binding. Additionally, the compound exhibited the highest negative ΔG = -7.2, indicating a strong and effective inhibition of the enzyme.[25]

Cyclooxygenase-2 (Cox-2) Concentration Level

Based on the results, a noteworthy elevation, at a probability level of P≤0.05, in the concentration of Cox-2 was evident among BBN-induced mice when compared to the control group. This increase can be attributed to the activation of signaling pathways within bladder cancer cells, which prompts the production and release of Cox-2.[26] The presence of chronic inflammation within the bladder, often associated with conditions like recurrent urinary tract infections or bladder stones, may contribute to enhanced Cox-2 expression. Inflammatory signals released during this process can stimulate the production of Cox-2.27]. Additionally, the results revealed

a significant decrease in Cox-2 concentration among mice treated with various doses as shown in Table 4, particularly A, B, C, and D, in comparison to the BBN-induced group due to interaction and inhibition of the enzyme form as shown in Figures 6-9. The notable decrease in Cox-2 concentration can be attributed to the remarkable efficacy of compound B doses as shown in Figure 7 when compared to the other treatments due to the strong interactions between the compound and the enzyme, as theoretically predicted by the docking program, there are four hydrogen bonds, along with other types of bonds, contributing to this strong binding. Additionally, the compound exhibited the highest negative ΔG= -7.9, indicating a strong and effective inhibition of the enzyme.[28]

Interleucein-6 (IL-6) Concentration Level

Based on the results, a significant increase at a probability level of P≤0.05 in IL-6 concentration was observed in BBN-induced mice compared to the control group as shown in Table 3. This may be due to can be attributed to the activation of signaling pathways within bladder cancer cells, leading to the production and release of IL-6. This can be influenced by genetic alterations or abnormalities in the cancer cells.[29] Additionally, the tumor microenvironment plays a crucial role in cancer development, and immune cells or other stromal cells within the bladder tumor can produce IL-6 or induce its production.[30] The results also show a significant decrease in mice treated with several doses such as A, B, C, and D compared to the BBN-induced group. The reason for this significant decrease in IL-6 concentration is due to strong binding and inhibition forms. The results showed that compound B doses were more effective compared to the others, a significant decrease has been observed as shown in Figure 7. The reason for this decrease is attributed to the strong binding interactions between the compound and the enzyme, as theoretically predicted by the docking program. There are four hydrogen bonds, along with other bonds, contributing to this strong binding. Additionally, the compound exhibited the highest negative ΔG = -7.4, indicating a strong and effective inhibition of the enzyme.[31]

Histological study

A histological study of rat bladder treated with (BBN) and new synthetic compounds.

First group

showed results indicating a normal state of the bladder. The mucosal layer and submucosal layer were observed to be intact with clear boundaries and no damage. Additionally, the transitional epithelial cells were present in their usual form, and the muscular layer also appeared normal without any observed damage as seen in diseased conditions. in Figures 10 and 11.

Second group

On the other hand, exhibited significant and noticeable tissue changes due to the administration of (BBN). These changes were characterized by the appearance of stenosis of the lumen with necrosis and sloughing of the transitional epithelium cells, thickening of the muscular, and infiltration of inflammatory cells, as depicted in Figures 12 and 13.

Third group

This group was dosed with (BBN) and then treated with (A) for 21 days. The results of the histological examination showed that the tissues were free of any form of damage when compared to the bladder of the second group, and the appearance singular degeneration and necrosis of the epithelial cells and mild thinning of the mucosa and mild infiltration of inflammatory cells, meaning that the treatment has a clear effect as shown in Figures 14 and 15.

Fourth group

the animals of this group were dosed with (BBM) and then treated with (B) for 21 days, and the response to this treatment

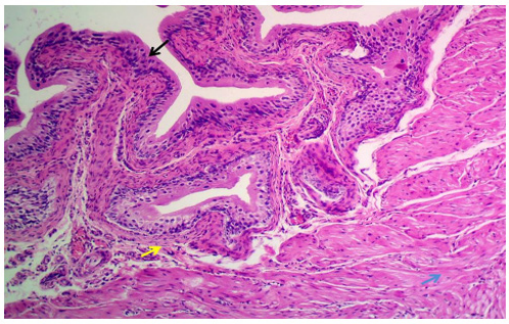

Figure 10: Histological section of mice urinary bladder of the Negative control group showing the normal architecture of the layers representing by mucosa lined with transitional epithelium cells (Black arrow), submucosa (Yellow arrow), and muscularis (Blue arrow). H&E stain, 100X.

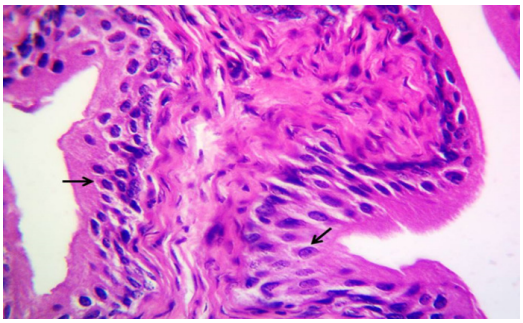

Figure 11: Histological section of mice urinary bladder of the Negative control group showing the normal architecture of the layers represented by mucosa lined with transitional epithelium cells (Black arrow). H&E stain, 400X.

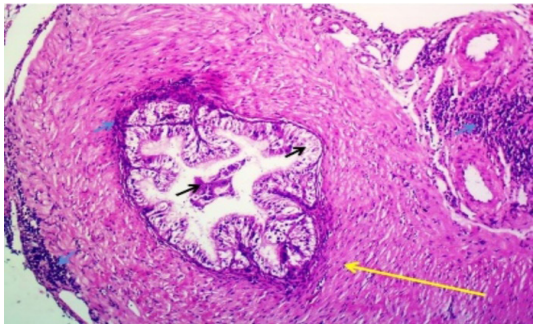

Figure 12: Histological section of mice urinary bladder of the positive control (infected) group showing stenosis of the lumen with necrosis and sloughing of the transitional epithelium cells (Black arrow), thickening of the muscular is (Yellow arrow), and infiltration of inflammatory cells (Blue H&E)

was very good in a theoretical and practical study, showing the normal architecture of the layers representing by mucosa lined with transitional epithelium cells and, submucosa and muscular is similar to the first group with a complete absence of any form of damage that occurred on the bladder tissue, meaning that the treatment was effective on the disease in a large and clear way, as shown in Figures 16 and 17.

Fifth group

animals of this group were dosed with (BBN) and then treated with (C) for 21 days, and its results showed that the repair process of bladder tissues had occurred, showing mild thinning of the mucosa and, mild focal infiltration of inflammatory cells in the submucosa and singular degeneration and necrosis of the

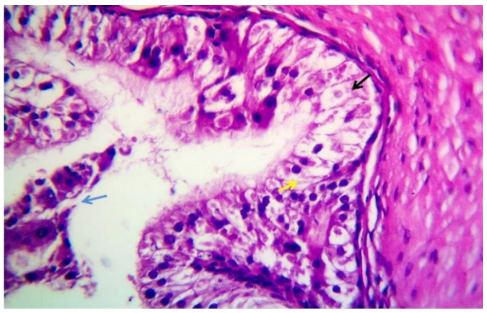

Figure 13: Histological section of mice urinary bladder of the positive control (infected) group showing necrosis (Black arrow), degeneration (Yellow arrow) and sloughing (Blue arrow) of the transitional epithelium cells, thickening of the muscular is, and infiltration of inflammatory cells H&E stain, 400 X.

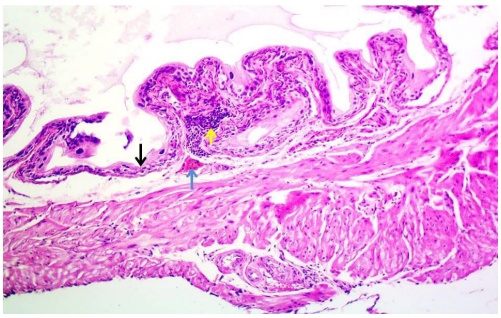

Figure 14: Histological section of mice urinary bladder of the treated A group showing mild thinning of the mucosa (Black arrow), mild infiltration of inflammatory cells (Yellow arrow), and edema (Blue arrow) H&Estain, 1 0 0 X.

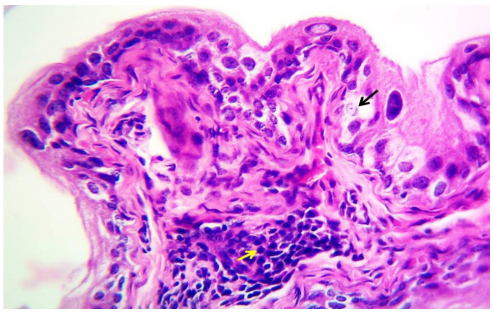

Figure 15: Histological section of mice urinary bladder of the treated A group showing singular degeneration and necrosis of the epithelial cells (Black arrow), mild infiltration of inflammatory cells (Yellow H&E stain, 4 0 0 X.

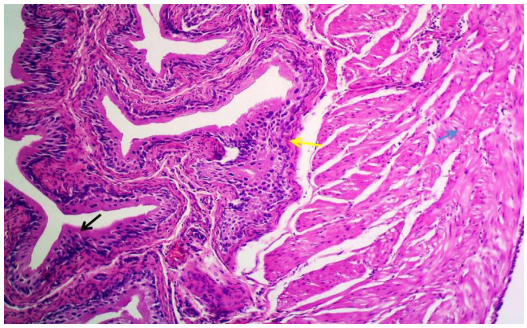

Figure 16: Histological section of mice urinary bladder of the treated B group showing the normal architecture of the layers represented by mucosa lined with transitional epithelium cells (Black arrow), submucosa (Yellow arrow), and muscular (Blue arrow). H&E stain, 100X.

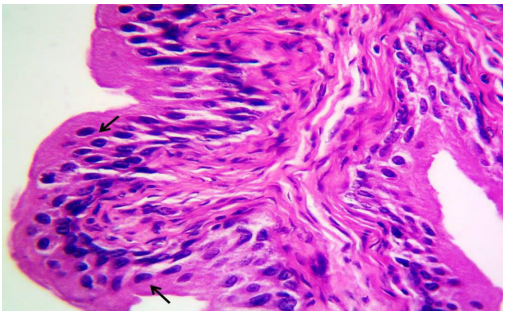

Figure 17: Histological section of mice urinary bladder of the treated B group showing the normal architecture of the layers represented by mucosa lined with transitional epithelium cells (Black arrow). H&E stain, 400X.

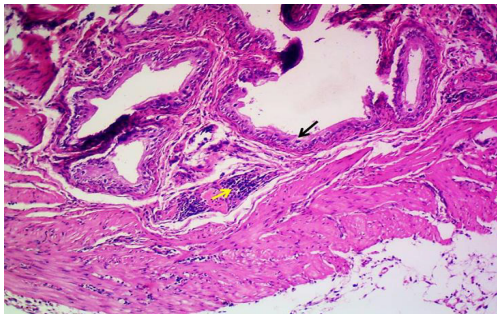

Figure 18: Histological section of mice urinary bladder of the treated C group showing mild thinning of the mucosa (Black arrow), mild focal infiltration of inflammatory cells in the submucasa (Yellow arrow), and edema (Blue arrow). H&E stain, 100X.

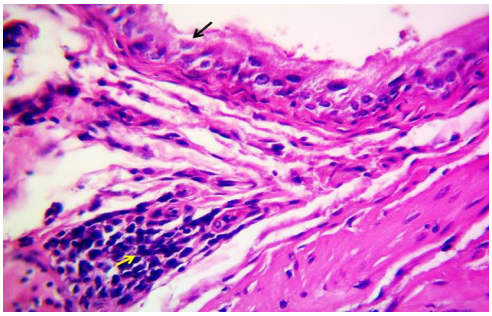

Figure 19: Histological section of mice urinary bladder of the treated C group showing singular degeneration and necrosis of the epithelial cells (Black arrow), mild infiltration of inflammatory cells (Yellow arrow). H&E stain, 400X.

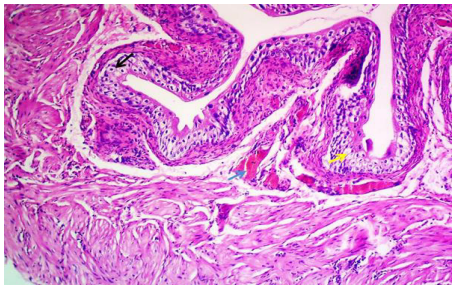

Figure 20: Histological section of mice urinary bladder of the treated D group showing severe vacuolar degeneration (Black arrow) and mild necrosis of the transitional epithelial cells (Yellow arrow), and congestion of blood vessels (Blue arrow). H&E stain, 100X.

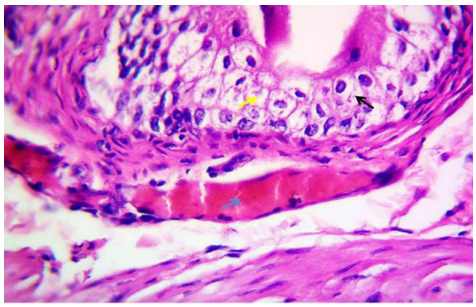

Figure 21: Histological section of mice urinary bladder of the treated D group showing severe vacuolar degeneration (Black arrow) and mild necrosis of the transitional epithelial cells (Yellow arrow), and congestion of blood vessels (Blue arrow). H&E stain, 400X.

epithelial cells, where they appeared clear treatment efficacy as shown in Figures 18 and 19.

Group Six

Animals in the sixth group were dosed with (BBN) to induce bladder damage and then treated with (D) for 21 days. The response to this treatment was good, showing severe vacuolar degeneration, mild necrosis of the transitional epithelial cells, and congestion of blood vessels. This indicates the effectiveness of the treatment compared to a secondary stage, as shown in Figures 20 and 21.

ACKNOWLEDGEMENT

First and foremost, I express my gratitude to the Almighty for granting me the strength and perseverance to complete this research. I sincerely thank my supervisor, Prof. Adnan O. Omar, for his unwavering support, guidance, and encouragement throughout this journey. His expertise and mentorship have been instrumental in shaping this work. I am deeply thankful to Mosul University, the Department of Chemistry, the College of Science, and the Department of Veterinary Medicine for providing the necessary facilities and resources to conduct animal experiments. Special appreciation goes to Assistant Professor Dr. Mohammed Bahry Hassin for his valuable advice and constructive feedback on the animal experiments. I would like to thank my family and friends for their constant encouragement, understanding, and support. Finally, I want to dedicate a special thank you to my mother, whose unwavering belief in me has driven my determination. Thank you all for being an essential part of this journey and for making this research possible.

REFERENCES

1. Khalaf KA, Omar AO. Green Synthesis and Spectroscopic Study of New Heterocyclic Compounds Derived from Ethyl Coumarilate. African Journal of Advanced Pure and Applied Sciences (AJAPAS). 2023 Jun 8:281-9.
2. D'arcy MS. Cell death: a review of the major forms of apoptosis, necrosis and autophagy. Cell biology international. 2019 Jun;43(6):582-92.
3. Ma J, Waxman DJ. Combination of antiangiogenesis with chemotherapy for more effective cancer treatment. Molecular cancer therapeutics. 2008 Dec 1;7(12):3670-84.
4. Makovec T. Cisplatin and beyond: molecular mechanisms of action and drug resistance development in cancer chemotherapy. Radiology and oncology. 2019 Mar 28;53(2):148-58.
5. Thoeny HC, Ross BD. Predicting and monitoring cancer treatment response with diffusion-weighted MRI. Journal of Magnetic Resonance Imaging. 2010 Jul;32(1):2-16.
6. Napiórkowska M, Cieślak M, Kaźmierczak-Barańska J, Królewska-Golińska K, Nawrot B. Synthesis of new derivatives of benzofuran as potential anticancer agents. Molecules. 2019 Apr 18;24(8):1529.
7. Abedinifar F, Farnia SM, Mahdavi M, Nadri H, Moradi A, Ghasemi JB, Küçükkılınç TT, Firoozpour L, Foroumadi A. Synthesis and cholinesterase inhibitory activity of new 2-benzofuran carboxamide-benzylpyridinum salts. Bioorganic Chemistry. 2018 Oct 1;80:180-8.
8. Kossakowski J, Krawiecka M, Kuran B, Stefańska J, Wolska I. Synthesis and preliminary evaluation of the antimicrobial activity of selected 3-benzofurancarboxylic acid derivatives. Molecules. 2010 Jul 6;15(7):4737-49.
9. Sehgal SA. Pharmacoinformatics and molecular docking studies reveal potential novel Proline Dehydrogenase (PRODH) compounds for Schizophrenia inhibition. Medicinal Chemistry Research. 2017 Feb;26:314-26.
10. Jiang Q, Matsuzaki Y, Li K, Uitto J. Transcriptional regulation and characterization of the promoter region of the human ABCC6 gene. Journal of investigative dermatology. 2006 Feb 1;126(2):325-35.
11. Madhuri ML, Reddy RR. In vitro Evaluation and Molecular Docking Analysis of Potential Anticancer Compounds from Syzygium alternifolium. International Research Journal of Pure and Applied Chemistry. 2022 Nov 23;23(6):1-8.
12. Ladokun OA, Abiola A, Okikiola D, Ayodeji F. GC-MS and molecular docking studies of Hunteria umbellata methanolic extract as a potent anti-diabetic. Informatics in Medicine Unlocked. 2018 Jan 1;13:1-8.
13. Odhar–E-mail HA, Hashim–E-mail AF, Ahjel–E-mail SW, Humadi–E-mail SS. Molecular docking and dynamics simulation analysis of the human FXIIa with compounds from the Mcule database. Bioinformation. 2023;19(2):160-6.
14. Kozlecki T, Samyn C, Alder RW, Green PG. Unexpected reactions of α, β-unsaturated esters with hydrazine hydrate. Journal of the Chemical Society, Perkin Transactions 2. 2001(2):243-6.
15. Jasinski JP, Golen JA, Samshuddin S, Narayana B, Yathirajan HS. Synthesis, characterization and crystal structures of 3, 5-bis (4-fluorophenyl)-4, 5-dihydro-1 H-pyrazole-1-carboxamide and 3, 5-bis (4-fluorophenyl)-4, 5-dihydro-1 H-pyrazole-1-carbothioamide. Crystals. 2012 Aug 15;2(3):1108-15.

16. Helali A, Al-Ghulikah H. Synthesis of some Heterocyclic Compound Using α, β-unsaturated Ketones. Journal of Advanced Pharmacy Research. 2019 Jan 1;3(1):35-46.
17. Hamdoon AM, Saleh MY, Saied SM. Synthesis & Biological Evaluation of Novel Series of Benzo [f] indazole Derivatives. Egyptian Journal of Chemistry. 2022 Nov 1;65(11):305-12.
18. Ajani OO, Isaac JT, Owoeye TF, Akinsiku AA. Exploration of the chemistry and biological properties of pyrimidine as a privilege pharmacophore in therapeutics. Int. J. Biol. Chem. 2015;9(4):148-77.
19. Soltani N, Behpour M, Oguzie EE, Mahluji M, Ghasemzadeh MA. Pyrimidine-2-thione derivatives as corrosion inhibitors for mild steel in acidic environments. RSC Advances. 2015;5(15):11145-62
20. Sagara Y, Miyata Y, Nomata K, Hayashi T, Kanetake H. Green tea polyphenol suppresses tumor invasion and angiogenesis in N-butyl-(-4-hydroxybutyl) nitrosamine-induced bladder cancer. Cancer epidemiology. 2010 Jun 1;34(3):350-4.
21. Erhirhie EO, Ekene NE, Ajaghaku DL. Guidelines on dosage calculation and stock solution preparation in experimental animals' studies. Journal of Natural Sciences Research. 2014;4(18):100-6.
22. Brown AM. A new software for carrying out one-way ANOVA post hoc tests. Computer methods and programs in biomedicine. 2005 Jul 1;79(1):89-95.
23. Yang T, Shi R, Chang L, Tang K, Chen K, Yu G, Tian Y, Guo Y, He W, Song X, Xu H. Huachansu suppresses human bladder cancer cell growth through the Fas/Fasl and TNF-alpha/TNFR1 pathway in vitro and in vivo. Journal of Experimental & Clinical Cancer Research. 2015 Dec;34:1-0.
24. Ronca R, Van Ginderachter JA, Turtoi A. Paracrine interactions of cancer-associated fibroblasts, macrophages and endothelial cells: tumor allies and foes. Current Opinion in Oncology. 2018 Jan 1;30(1):45-53.
25. Baldisserotto A, Demurtas M, Lampronti I, Moi D, Balboni G, Vertuani S, Manfredini S, Onnis V. Benzofuran hydrazones as potential scaffold in the development of multifunctional drugs: Synthesis and evaluation of antioxidant, photoprotective and antiproliferative activity. European journal of medicinal chemistry. 2018 Aug 5;156:118-25.
26. Adhim Z, Matsuoka T, Bito T, Shigemura K, Lee KM, Kawabata M, Fujisawa M, Nibu K, Shirakawa T. In vitro and in vivo inhibitory effect of three Cox-2 inhibitors and epithelial-to-mesenchymal transition in human bladder cancer cell lines. British journal of cancer. 2011 Jul;105(3):393-402.
27. Keibel A, Singh V, Sharma MC. Inflammation, microenvironment, and the immune system in cancer progression. Current pharmaceutical design. 2009 Jun 1;15(17):1949-55.
28. He X, Gao Y, Hui Z, Shen G, Wang S, Xie T, Ye XY. 4-Hydroxy-3-methylbenzofuran-2-carbohydrazones as novel LSD1 inhibitors. Bioorganic & Medicinal Chemistry Letters. 2020 May 15;30(10):127109.
29. Chen MF, Lin PY, Wu CF, Chen WC, Wu CT. IL-6 expression regulates tumorigenicity and correlates with prognosis in bladder cancer. PLoS One. 2013 Apr 30;8(4):e61901.
30. Hatogai K, Sweis RF. The tumor microenvironment of bladder cancer. Tumor Microenvironments in Organs: From the Brain to the Skin–Part B. 2020:275-90.